• Article •

Causal propagation of signals in strangeon matter

JiGuang Lu[1,2*], EnPing Zhou[3], XiaoYu Lai[4,5], and RenXin Xu[3,6]

[1]*CAS Key Laboratory of FAST, National Astronomical Observatories, Chinese Academy of Sciences, Beijing 100012, China;*
[2]*Key Laboratory of Radio Astronomy, Chinese Academy of Sciences, Beijing 100012, China;*
[3]*School of Physics and State Key Laboratory of Nuclear Science and Technology, Peking University, Beijing 100871, China;*
[4]*School of Physics and Mechanical & Electrical Engineering, Hubei University of Education, Wuhan 430205, China;*
[5]*Xinjiang Astronomical Observatory, Chinese Academy of Sciences, Urumqi 830011, China;*
[6]*Kavil Institute for Astronomy and Astrophysics, Peking University, Beijing 100871, China*

The state equation for strangeon matter is very stiff due to the non-relativistic nature of its particles and their repulsive interaction, such that pulsar masses as high as $\sim 3M_\odot$ would be expected. However, an adiabatic sound speed, $c_s = \sqrt{\partial P/\partial \rho}$, is usually superluminal in strangeon matter, and the dynamic response of a strangeon star (e.g., binary merger) is not tractable in numerical simulations. In this study, we examined signal propagation in strangeon matter and calculate the actual propagation speed, c_{signal}. We found that the causality condition , $c_{\text{signal}} < c$, is satisfied and the signal speed is presented as a function of stellar radius.

1 Introduction

Understanding the nature of pulsars depends on an understanding of the state of supranuclear matter, which is related to the non-perturbative behavior of fundamental strong interactions. Even though more than half a century passed after its discovery, this topic remains poorly understood. In the era of gravitational wave astronomy, however, this state may soon be understood, especially after the GW170817 event caused by the merger of binary compact stars [1]. This type of event can certainly help to distinguish the equation of state (EoS) models of a compact star (see ref. [2] for a review). In fact, the post-merger gravitational wave signal and its electromagnetic counterparts are closely related to the shocks and ejected material

accompanying the merger of binary compact stars, whereas the dynamical response depends on the sound speed in compact star matter [3]. Of course, sound speed depends on the EoS of compact star matter. As such, it is essential to properly calculate the sound speed in order to study the mergers of binary compact stars with numerical relativity.

Although there is not yet a good understanding of quantum chromodynamics at low energy scales, there have been many speculations about the EoS of cold supranuclear-density matter and about so-called strange matter. This idea says that 3-flavored strange matter (composed of free *u*, *d* and *s* quarks) could be even more stable than 2-flavored nucleon matter [4,5]. Based on this, various models for 3-flavored strange stars are being considered. The widely used Massachusetts Institute of Technology bag model (MIT) bag model, which treats quarks as free and relativistic, was often adopted to describe the matter state of pulsars [6, 7]. In this case, the max-

imum mass of a pulsar can barely reach $2 M_\odot$. Then, the observation of the $1.97 M_\odot$ pulsar J0715+1807 [8] and $2.01 M_\odot$ pulsar J0348+0432 [9] marginally ruled out this quark star model. In fact, even in the neutron star model, $2 M_\odot$ is still too large to consider due to the "hyperon puzzle" [10, 11]. Another strange matter model in which the quarks are bound in clusters (formerly known as strange quark-clusters [12], which are like nucleons but with strange quarks, hereafter, strangeons [13]) allows the maximum mass of a pulsar to be much larger [14]. Therefore, the strangeon star model is more favorable than others in comprehending the mass of pulsars. In addition, the strangeon star model can also solve some problems that are difficult to address in other models, e.g., bi-drifting of sub-pulses [15], the non-atomic feature in the spectrum of X-ray dim isolated neutron stars (XDINSs) [16], two types of glitches in normal pulsars and AXP/SGRs [17], and the optical/UV excess of XDINSs [18].

However, the strangeon star model is sometimes rejected because its matter state is too stiff. Based on the conventional formula, the sound speed $c_s = \sqrt{\partial P/\partial \rho}$ in such stiff matter would exceed even the speed of light [19-22], so the maximum mass of a compact star would never be larger than $3.2 M_\odot$ [23]. Obviously, the maximum mass of a strangeon star conflicts with the above result [14, 24, 25]. In fact, Caporaso and Brecher [26] pointed out that it is possible to construct a lattice model with $\partial p/\partial \rho > c^2$ and a subluminal signal speed. However, their work assumed electromagnetic interaction and did not include the expression of signal speed. Here, we put forward a signal speed for a more general case, which can at least be correctly adopted in strangeon matter and is absolutely necessary for simulating a strangeon star merger [27] with numerical relativity.

A strangeon is much more massive than a nucleon. Therefore, in matter with similar mass density, the quantum wave packet of a particle in strangeon matter is smaller than that in nucleon matter. Thus, the strangeon could be regarded as a classical localized particle rather than a quantum wave packet. In this paper, for the sake of simplicity, we consider oscillation propagation in a 1-D discrete chain. In sect. 2, we theoretically derive the sound speed in a 1-D chain of particles and we discuss this speed in sect. 3. We summarize our results in sect. 4.

2 A model to calculate signal speed

Consider a 1-D chain of particles, in which the particles along the chain can vibrate slightly. The position of the n-th particle can be expressed as a function of time t, as follows:

$$x_n = f(n, t) + l(n), \tag{1}$$

where $l(n)$ is the average position of the n-th particle and $f(n, t)$ is its relative displacement, which has a zero mean. Assume a two-body short-range (which means the interaction affects only nearby particles) repulsive conservative interaction $F(x)$, which is related only to the distance between two particles x. Then, the force on the n-th particle by the subsequent or previous particle can be expressed as follows:

$$F_{n+} = F(|x_{n+1,\,\text{ret}} - x_n|), \quad F_{n-} = F(|x_{n-1,\,\text{ret}} - x_n|), \tag{2}$$

where the subscript "ret" indicates that this is a retarding force because of the propagation of the force field. In this paper, we assume that the propagation speed of the force field is the speed of light c. With the assumption of small amplitude, $f(n, t),\ f(n - 1, t) \ll l(n) - l(n - 1)$, we can expand the force to the first order of the distance between particles at their average position.

$$F_{n+} = F\left(f\left(n + 1, t - \frac{l(n + 1) - l(n)}{c}\right) - f(n, t)\right.$$
$$\left. + [l(n + 1) - l(n)]\right)$$
$$\approx F(l(n + 1) - l(n)) + \left[f\left(n + 1, t - \frac{l(n + 1) - l(n)}{c}\right)\right.$$
$$\left. - f(n, t)\right]\frac{\partial F}{\partial x}\Bigg|_{x=l(n+1)-l(n)}, \tag{3}$$

$$F_{n-} = F\left(f(n, t) - f\left(n - 1, t - \frac{l(n) - l(n - 1)}{c}\right)\right.$$
$$\left. + [l(n) - l(n - 1)]\right)$$
$$\approx F(l(n) - l(n - 1)) + \left[f(n, t)\right.$$
$$\left. - f\left(n - 1, t - \frac{l(n) - l(n - 1)}{c}\right)\right]\frac{\partial F}{\partial x}\Bigg|_{x=l(n)-l(n-1)}. \tag{4}$$

On the other hand, the resultant force on the n-th particle can be expressed as follows:

$$F_n = \frac{\mathrm{d}^2 f}{\mathrm{d}t^2} = F_{n-} - F_{n+}$$
$$\approx F(l(n) - l(n - 1)) - F(l(n + 1) - l(n))$$
$$+ \left[f(n, t) - f\left(n - 1, t - \frac{l(n) - l(n - 1)}{c}\right)\right]\frac{\partial F}{\partial x}\Bigg|_{x=l(n)-l(n-1)}$$
$$- \left[f\left(n + 1, t - \frac{l(n + 1) - l(n)}{c}\right) - f(n, t)\right]\frac{\partial F}{\partial x}\Bigg|_{x=l(n+1)-l(n)}, \tag{5}$$

where m is the mass of each particle. Taking the average of eq. (5), we can obtain $F(l(n) - l(n - 1)) - F(l(n + 1) - l(n)) = 0$. The repulsive interaction is generally monotonous with distance x (over a small range), which means that $l(n) - l(n - 1) = l(n + 1) - l(n)$, i.e., the interparticle spacing is regular. This constant is represented as l below.

To calculate the sound speed, first, we consider the wave propagation process in the frequency domain, as in the traditional method.

2.1 Frequency-domain oscillation propagation in an infinite chain

In the frequency domain, eq. (5) can be expressed as follows:

$$\frac{g(n+1,\omega) + g(n-1,\omega)}{g(n,\omega)} = 2\left(1 - \frac{m\omega^2}{2\frac{\partial F}{\partial x}\big|_{x=l}}\right)\exp\left(i\frac{l\omega}{c}\right), \quad (6)$$

where $g(n,\omega)$ is the complex amplitude of the n-th particle at frequency ω, and $\frac{\partial F}{\partial x}\big|_{x=l} \approx -3(1-2\nu)\frac{m}{l^2}\left(\frac{\partial P}{\partial \rho}\right)_T$, P and ρ are the internal pressure and density of the chain, respectively, ν is the Poisson's ratio, and the subscript T indicates that the derivative is taken isothermally. Considering that the Poisson's ratio for a perfectly isotropic elastic material is 0.25 and the adiabatic index of the 1-D matter discussed here is 3 (degree of freedom is 1), the $\frac{\partial F}{\partial x}\big|_{x=l}$ can be expressed as $-\frac{m}{2l^2}\left(\frac{\partial P}{\partial \rho}\right)_S$, where the subscript S indicates that the derivative is taken isentropically. The stable solution for eq. (6) is as follows (in which the divergent branch is abandoned):

$$\frac{g(n+1,\omega)}{g(n,\omega)} = b - \sqrt{b^2 - 1}, \quad (7)$$

where $b = \left[1 - \frac{l^2\omega^2}{\left(\frac{\partial P}{\partial \rho}\right)_S}\right]\exp\left(i\frac{l\omega}{c}\right)$. With the phase variation shown in the above equation, we can calculate the apparent phase and group velocities of the oscillation as follows:

$$c_p = \frac{l\omega}{-\arg\left[\frac{g(n+1,\omega)}{g(n,\omega)}\right]}, \quad (8)$$

$$c_g = \frac{c_p^2}{c_p - \omega\frac{dc_p}{d\omega}}. \quad (9)$$

As shown in eq. (7), the amplitude of the oscillation dampens while propagating, which implies that there is reflection wave in the chain. In this case, neither the phase velocity nor group velocity represents the velocity of the signal propagation. Hence, we must calculate the signal propagation in the time domain.

2.2 Time-domain impulse response in finite chain

Here, we consider the transfer function of the system in which a signal propagates in a 1-D chain with k particles. eq. (5) shows that the acceleration of each particle (i.e., the second time derivative of the particle's displacement) is affected by its own position and that of nearby particles, and that the whole system is linearly time-invariant. Figure 1 shows a block diagram of this system, in which each node represents the displacement of each particle x_n, D is the delay element with the transfer function $D(s) = \exp\left(-\frac{ls}{c}\right)$, G_0 is the proportional derivative element with the transfer equation $G_0(s) = -\frac{1}{ms^2}\frac{\partial F}{\partial x}\big|_{x=l}$, and s is the complex variable (or complex frequency) corresponding to the Laplace transform of $f(t)$

$$T_n(s) = \mathscr{L}[f(t)] = \int_0^\infty f(n,t)\exp(-st)dt. \quad (10)$$

In Figure 1, each feedback branch with a multiplicative gain of "–2" represents the effect of the particle position on its own acceleration, and the multiplicative gain of "+" is the effect of the posterior particle. A feedback of "–2" of the last particle indicates that the last particle is limited by the rigid boundary. Since the element composed of a delay element and a feedback loop repeats n times in the block diagram, the diagram can be simplified as shown in Figure 2, where

$$G_1(s) = \frac{G_0 D}{1 + 2G_0}. \quad (11)$$

Using Mason's gain formula, the total transfer function of the system can be obtained as follows:

$$G(s) = \frac{G_1^k}{\sum_{m=0}^{\lfloor\frac{k}{2}\rfloor} C_{k-m}^m (-G_1^2)^m} = \frac{2^k G_1^k}{k + 1 + O[1 - 4G_1^2]}. \quad (12)$$

With the low frequency assumption $l\omega \ll \min\left(c, \sqrt{\left(\frac{\partial P}{\partial \rho}\right)_S}\right)$, we can approximate the transfer function at a short-range $(1 \ll k \ll \left(\frac{\partial P}{\partial \rho}\right)_S \frac{1}{l^2\omega^2})$ as follows:

$$G(s) = \frac{2^k G_1^k}{k+1} = \frac{1}{k+1}\left[\frac{\left(\frac{\partial P}{\partial \rho}\right)_S}{l^2 s^2 + \left(\frac{\partial P}{\partial \rho}\right)_S}\right]^k \exp\left(-\frac{kls}{c}\right). \quad (13)$$

Thus, for an impulse signal $x_0(t) = A\delta(t)$, the response should be

$$\begin{aligned} x_k(t) &= \mathscr{L}^{-1}[\mathscr{L}[x_0(t)]G(s)] \\ &= \frac{2^{k-\frac{1}{2}}\sqrt{\pi}A}{(k+1)\Gamma(k)}\sqrt{\frac{1}{l^2}\left(\frac{\partial P}{\partial \rho}\right)_S}\,\theta^{k-\frac{1}{2}}J_{k-\frac{1}{2}}(\theta), \end{aligned} \quad (14)$$

where $\theta = \sqrt{\frac{1}{l^2}\left(\frac{\partial P}{\partial \rho}\right)_S}\left(t - \frac{kl}{c}\right)$, Γ is the Gamma function and J is the Bessel function of the first kind. The position of the first maximum point of eq. (14) provides the propagation time of the signal (here, we regard the peak time as the propagation time). Considering the relation [28]

$$\frac{d[\theta^\nu J_\nu(\theta)]}{d\theta} = \theta^\nu J_{\nu-1}(\theta), \quad (15)$$

and the asymptotic about the first zeros of the Bessel function
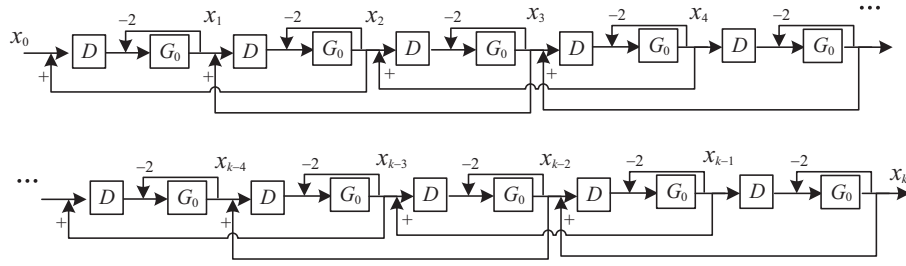
Figure 1   Block diagram of signal propagation. Each node represents the displacement of each particle in the chain, with D as the delay element and G_0 as the proportional derivative element.
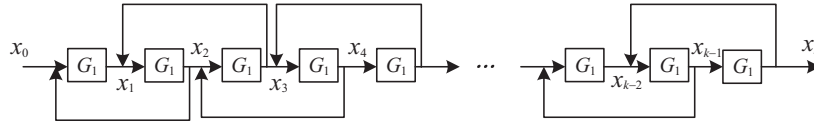
Figure 2   Simplified block diagram of signal propagation. G_1 is the proportional derivative element.

$j_{\nu 1}$ [29]

$$j_{\nu 1} = \nu + 1.855757\nu^{1/3} + 1.003315\nu^{-1/3} + O[\nu^{-1}], \qquad (16)$$

we can obtain the signal propagation time, as follows:

$$t_{\text{signal}} = \frac{k - \frac{3}{2} + 1.855757\left(k - \frac{3}{2}\right)^{1/3} + O[1]}{\sqrt{\frac{1}{l^2}\left(\frac{\partial P}{\partial \rho}\right)_S}} + \frac{kl}{c}. \qquad (17)$$

Finally, the signal propagation speed should take the following form (for $k \gg 1$):

$$c_{\text{signal}} = \frac{kl}{t_{\text{signal}}} \approx \frac{1}{\frac{1}{\sqrt{\left(\frac{\partial P}{\partial \rho}\right)_S}} + \frac{1}{c}} < c. \qquad (18)$$

If we ignore the propagation delay of the force field, i.e., $c_{\text{signal}} \approx \sqrt{\left(\frac{\partial P}{\partial \rho}\right)_S}$, the result is actually the conventional sound speed. eq. (18) also implies that the signal propagation can never be faster than light, as shown in Figure 3.

We should also note that the speed we use here is the average speed, which is just derived from the output signal (the displacement of the last particle). In fact, here, we do not derive the movement of the particles other than those at both ends of the chain.

2.3   Signal propagations inside star

Based on the derivation in sect. 2.2, the signal propagation speed c_{signal} in strangeon matter is always slower than the speed of light. With a definite EoS, we can obtain the c_{signal} value in a strangeon star as well. Here, we adopt the EoS supplied by Lai and Xu [14], and Figure 4 shows the corresponding c_{signal} in a strangeon star. It could be shown that
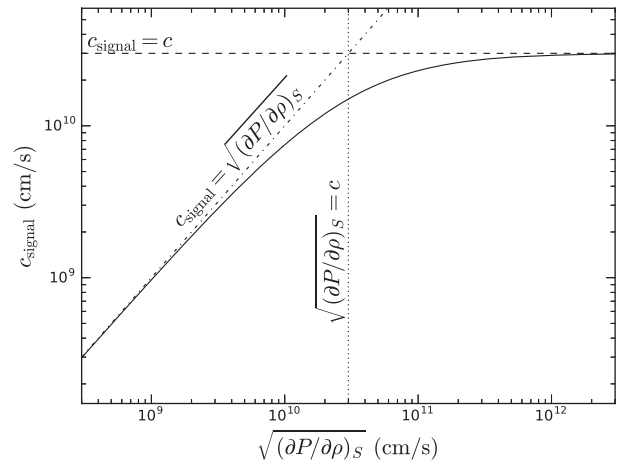
Figure 3   Relation between signal speed c_{signal} and $\sqrt{\left(\frac{\partial P}{\partial \rho}\right)_S}$.
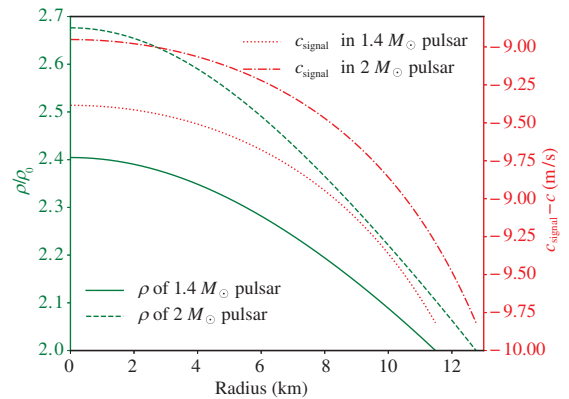
Figure 4   (Color online) Density ρ and signal speed c_{signal} in strangeon stars, where ρ_0 is the nuclear matter density. We calculate the density of a strangeon star using the EoS supplied by ref. [14].

the c_{signal} in a strangeon star is quite close to c, and c_{signal} decreases from the stellar center to the surface with the density. Therefore, it would be a good approximation to assume a kinematic perturbation in the strangeon matter responses at the speed of light, c, because the real one deviates by only $\sim 10^{-8}c$.

3 Discussion

3.1 Assumptions in the derivation

We made a few assumptions in this derivation and discuss the applicability of these assumptions below.

3.1.1 Small amplitude assumption

The assumption of small amplitude is made throughout the derivation process. In fact, in traditional derivations of sound speed, small amplitude assumption is also adopted to ensure the linearity of the system, but here it is much stricter. Small amplitude here means that the amplitude is much smaller than the interparticle spacing, which is violated in most cases. Actually, this assumption can be replaced by a stable spacing assumption, $f(n + 1, t) - f(n, t) \ll [l(n + 1) - l(n)]$, i.e., the distance between nearby particles is almost invariant. This assumption is equivalent to the traditional small amplitude assumption (although it still does not apply to normal gas).

In the derivation, we assume the oscillation to be longitudinal. Nevertheless, the small amplitude assumption makes the derivation results also applicable to transverse waves. For a transverse wave, the repulsive force is replaced by an attractive force (the relation between this force and the tension in the chain also differs), and the position of each particle along the chain must be manually arranged in advance.

In a triaxial crystal, the potential in each lattice is also triaxial. With the small amplitude assumption, the potential near each particle can be approximated as the triaxial harmonic oscillator potential. While oscillation propagates along the axis of this potential (assuming a short range, this constraint ensures the degree of freedom to be 1), the derivations in sect. 2 are still available. The speed of a plane sound wave along different axes also differs, depending on the potential and the lattice constant. However, the oscillation whose propagation direction avoids the potential axis is so complex that we do not consider it in this paper.

3.1.2 Low frequency assumption

In the derivation, we assume the frequency to be low, $l\omega \ll \min\left(c, \sqrt{\left(\frac{\partial P}{\partial \rho}\right)_S}\right)$, for convenience. This assumption obviously conflicts with the input signal $x_0(t) = A\delta(t)$ in sect. 2.2,

but it does not affect the result. In real physics processes with continuous time, an impulse in the form of a Dirac delta function $\delta(t) = \frac{1}{2\pi} \int_{-\infty}^{\infty} \exp(i\omega t)\mathrm{d}\omega$ does not exist. A real impulse can be treated as a process only contains low-frequency components $\frac{1}{2\pi} \int_{-\omega_0}^{\omega_0} \exp(i\omega t)\mathrm{d}\omega$ with a very large cut-off frequency ω_0 (in compact matter, ω_0 can be as large as 10^{23} rad/s, which is similar to the frequency of a 100 MeV γ-ray). This implies that the low frequency assumption is reasonable.

In the derivation, although we adopt the retarding force, the potential field is delayed rather than the force in fact. The retarding potential not only affects the action time of the force, but also can affect its strength. With a low frequency assumption, the particle movement speed is far less than the speed of light, which means that we can ignore variations in the strength caused by the retarding potential.

In the longitudinal wave, the magnetic field caused by the movement of particles (if the particles are charged) has no effect, but in the transverse wave, the magnetic field can make a difference. With the low frequency assumption, however, this magnetic field is so weak that its effect can be ignored. Thus, the assumption of conservative force loses no efficacy.

Additionally, we can ignore the electromagnetic radiation. With the low frequency assumption, the variation in the field energy density is too weak, which leads us to use mass density instead of energy density in our derivation.

3.1.3 Short-range assumption

To simplify the equation, we adopt the "short-range" assumption, $k \ll \left(\frac{\partial P}{\partial \rho}\right)_S \frac{1}{l^2\omega^2}$. In fact, this "short-range" is not a short distance at all. For typical parameters in dense matter $\omega = 10^{10}$ rad/s, $l = 10^{-15}$ cm, and $\frac{\partial P}{\partial \rho} = 10^{20}$ (cm/s)^2, this limit is 10^{20} cm, which is much larger than the length scale of a compact star.

3.1.4 Rigid boundary assumption

In sect. 2.2, the rigid boundary assumption is adopted to limit the displacement of the last particle. In fact, this boundary condition can be replaced by others, e.g., the free boundary condition. For a free boundary, this assumption implies that the average point of each particle is also the force balance point, $F(x)\big|_{x=l} = 0$. In this case, the feedback of the last particle should be adjusted to "–". However, this would not significantly change the final sound speed.

3.2 Waveform variation

For a traditional sound wave, the waveform is invariant during propagation. But in the discrete medium, this is not so.

In the particle chain, the input signal $x_0(t)$ is restricted to being continuous, which implies that the strength of the force on other particles is continuous, i.e., the second time derivative of particle's displacement is continuous. But the input signal does not always have a continuous second time derivative, which means that the waveform could change while propagating. A variation in a waveform indicates that the sound speed varies with frequency. Thus, the sound wave dispersion is a corollary of a discrete medium.

In addition to the dispersion, even for a single frequency wave, the amplitude would vary, as shown in eq. (7). This effect is due to the retarding force. If the amplitude is assumed to be invariant, the total work of resultant force on each particle in one period would be nonzero. This means that a system with a sound wave with invariant amplitude is unstable, i.e., the amplitude of the sound wave must change. The amplitude variation does not mean that the energy dissipates; actually, the energy is simply reflected. As with the evanescent wave, the energy of a sound wave is reflected and its amplitude decreases.

As shown in eq. (14), the oscillation of the output signal becomes increasingly violent with time, and this is obviously unreasonable. In fact, this enhancement cannot occur because of the small amplitude assumption (although the input signal, $x_0(t) = A\delta(t)$, also violates this assumption). If the amplitude increases to a very large value, the system would become nonlinear and the derivation in sect. 2.2 would fail. In addition, the ringing after peak time is not overshot, because the amplitude of the Dirac delta function is infinity (as is its energy). We know that the Bessel function $J_\nu(\theta)$ oscillates at a large θ with a period 2π, so we can define a characteristic frequency of this system like the eigenfrequency $\omega_c = \sqrt{\frac{2}{l^2}\left(\frac{\partial P}{\partial \rho}\right)_S}$. This frequency describes the oscillation property of a chain and is also the limit of the "low frequency."

3.3   Sound speed and strangeon star

With the traditional sound speed formula, it has been proved that the mass of a neutron star should be less than $3.2\,M_\odot$ [23], and a "safe" upper limit for the mass of a neutron star, $2.9\,M_\odot$, can also be obtained [30]. But in strangeon matter, the sound speed no longer limits the matter state. As such, the maximum mass of a strangeon star could easily exceed $3.2\,M_\odot$, and can even be much higher.

This result may explain the "mass gap" puzzle. It was found that there could be "gap" between the least massive black hole and the upper limit mass for a neutron star [31]. The lower bound of the 1% quantile from each black hole mass distribution has also been shown to be about $4.3\,M_\odot$ [32]. With the strangeon star model, this puzzle could be explained if the maximum mass of a strangeon star can reach $\sim 4\,M_\odot$.

Also, the possibility of a value of $\partial P/\partial \rho$ larger than c^2 also results in quite a different tidal deformability of a strangeon star. For conventional nuclear EoSs, it's widely accepted that the asymptotic sound speed is smaller than $c/\sqrt{3}$ in ultra-high densities. By fixing an upper limit for $\partial P/\partial \rho$ accordingly, it has been shown that the maximum mass of an EoS model decreases as the tidal deformability decreases [33]. Similar arguments are made for conventional quark stars within the MIT bag model description and the consideration of a color-flavor-locked phase [34]. Since the strangeon star can have a $\partial P/\partial \rho$ value larger than c^2 without violating causality, its tidal deformability has been found to be compatible with the observation of GW170817 [1], although its maximum mass is very large [27].

4   Summary

In this paper, we calculated the oscillation propagation in a discrete medium in both the frequency and time domains and obtained the sound speed. Our results show that the signal propagation speed would never exceed the speed of light, and in the small $(\partial P/\partial \rho)_S$ case, its expression would degenerate to the traditional form of sound speed. Thus, the strangeon star model can be safely used without concern about its conflict with causality.

In the strangeon star model, the mass of pulsars can be much higher, which implies that more massive pulsars may be found, although the accurate mass of a pulsar is hard to measure. In future work, the five-hundred-meter aperture spherical radio telescope (FAST) may prove to be sufficiently sensitive to detect weaker radio signals from pulsars far away, and it could also provide higher precision timing results to obtain the accurate mass of pulsars [35]. The discovery of more massive pulsars is expected.

1   B. P. Abbott, et al. (LIGO Scientific Collaboration and Virgo Collaboration), Phys. Rev. Lett. **118**, 121102 (2017), arXiv: 1612.02030.

2   L. Baiotti, and L. Rezzolla, Rep. Prog. Phys. **80**, 096901 (2017), arXiv: 1607.03540.

3   L. Rezzolla, and O. Zanotti, in *Relativistic Hydrodynamics* (Oxford University Press, Oxford, 2013).

4   A. R. Bodmer, Phys. Rev. D **4**, 1601 (1971).

5   E. Witten, Phys. Rev. D **30**, 272 (1984).

6   C. Alcock, E. Farhi, and A. Olinto, Astrophys. J. **310**, 261 (1996).

7   P. Haensel, J. L. Zdunik, and R. Schaefer, Astron. Astrophys. **160**, 121 (1986).

8   P. B. Demorest, T. Pennucci, S. M. Ransom, M. S. E. Roberts, and J. W. T. Hessels, Nature **467**, 1081 (2010), arXiv: 1010.5788.

9   J. Antoniadis, P. C. C. Freire, N. Wex, T. M. Tauris, R. S. Lynch, M. H. van Kerkwijk, M. Kramer, C. Bassa, V. S. Dhillon, T. Driebe, J. W. T. Hessels, V. M. Kaspi, V. I. Kondratiev, N. Langer, T. R. Marsh, M. A. McLaughlin, T. T. Pennucci, S. M. Ransom, I. H. Stairs, J. van Leeuwen, J. P. W. Verbiest, and D. G. Whelan, Science **340**, 1233232 (2013), arXiv: 1304.6875.

10   J. Schaffner-Bielich, Nucl. Phys. A **804**, 309 (2008), arXiv: 0801.3791.

11   I. Bombaci, JPS Conf. Proc. **17**, 101002 (2017).

12   R. X. Xu, Astrophys. J. **596**, L59 (2003).

13   R. Xu, Sci. China-Phys. Mech. Astron. **61** (2018), arXiv: 1802.04465.

14   X. Y. Lai, and R. X. Xu, Mon. Not. R. Astron. Soc.-Lett. **398**, L31 (2009), arXiv: 0905.2839.

15   G. J. Qiao, K. J. Lee, B. Zhang, R. X. Xu, and H. G. Wang, Astrophys. J. **616**, L127 (2004).

16   J. G. Lu, R. X. Xu, and H. Feng, Chin. Phys. Lett. **30**, 059501 (2013), arXiv: 1302.1328.

17   E. P. Zhou, J. G. Lu, H. Tong, and R. X. Xu, Mon. Not. R. Astron. Soc. **443**, 2705 (2014), arXiv: 1404.2793.

18   W. Wang, J. Lu, H. Tong, M. Ge, Z. Li, Y. Men, and R. Xu, Astrophys. J. **837**, 81 (2017), arXiv: 1603.08288.

19   S. Bayin, Phys. Rev. D **21**, 1503 (1980).

20   S. A. Bludman, and M. A. Ruderman, Phys. Rev. **170**, 1176 (1968).

21   S. A. Bludman, and M. A. Ruderman, Phys. Rev. D **1**, 3243 (1970).

22   B. D. Keister, and W. N. Polyzou, Phys. Rev. C **54**, 2023 (1996).

23   C. E. Rhoades, and R. Ruffini, Phys. Rev. Lett. **32**, 324 (1974).

24   Y. J. Guo, X. Y. Lai, and R. X. Xu, Chin. Phys. C **38**, 055101 (2014).

25   X. Y. Lai, C. Y. Gao, and R. X. Xu, Mon. Not. R. Astron. Soc. **431**, 3282 (2013).

26   G. Caporaso, and K. Brecher, Phys. Rev. D **20**, 1823 (1979).

27   X. Y. Lai, Y. W. Yu, E. P. Zhou, Y. Y. Li, and R. X. Xu, Res. Astron. Astrophys. **18**, 24 (2018), arXiv: 1710.04964.

28   M. Abramowitz, and I. A. Stegun, eds, in *Handbook of Mathematical Functions*: *With Formulas*, *Graphs*, *and Mathematical Tables* (National Bureau of Standards, 1970).

29   F. G. Tricomi, Atti Accad. Sci. Torino Cl. Fis. Mat. Nat. **83**, 3 (1949).

30   V. Kalogera, and G. Baym, Astrophys. J. **470**, L61 (1996).

31   C. D. Bailyn, R. K. Jain, P. Coppi, and J. A. Orosz, Astrophys. J. **499**, 367 (1998).

32   W. M. Farr, N. Sravan, A. Cantrell, L. Kreidberg, C. D. Bailyn, I. Mandel, and V. Kalogera, Astrophys. J. **741**, 103 (2011), arXiv: 1011.1459.

33   E. Annala, T. Gorda, A. Kurkela, and A. Vuorinen, arXiv: 1711.02644.

34   E. P. Zhou, X. Zhou, and A. Li, arXiv: 1711.04312.

35   J. Lu, and R. Xu, Front. Radio Astron. FAST Early Sci. Symp. **502**, 35 (2016).